

## Chapter 14

# Excited states

After studying various approaches to describe the  $sp$  propagator in a many-fermion system in Chs. 11 and 13, it is now time to discuss the description of excited states of the system with  $A$  particles. In Sec. 14.1 the relevant limit of the  $tp$  propagator  $G_{II}$  will be introduced which is appropriate for the calculation of these excited states. While it is possible to develop all the details of the corresponding diagrammatic expansion of this so-called particle-hole (ph) or polarization propagator, it is assumed that the reader is now sufficiently familiar with this procedure so that a somewhat different approach will be developed here. This approach will be linked to the Hartree-Fock approximation to the  $sp$  propagator in Sec. 16.4. The resulting approximation to the polarization propagator is widely used and presented in Sec. 14.2. While the name for this procedure is not too illuminating at first, it is historically called the random phase approximation (RPA). In Sec. 14.3 a simple model is employed to illustrate the scope of the RPA in a finite system. Many of the observed properties of excited states in many-fermion systems can be interpreted in terms of this schematic model. Especially the appearance of collective states in relation to the character of the ph interaction, whether it is on average attractive or repulsive, can be illustrated fruitfully. Excited states of atoms are discussed in Sec. 14.4.

For infinite systems the calculation of the noninteracting ph propagator is presented in Sec. 14.5. This so-called Lindhard function exhibits various properties that are helpful in assessing the properties of excitations in infinite systems. The important collective state of the electron gas, known as the plasmon, is discussed in Sec. 14.6. The response of nuclear matter with quantum numbers corresponding to the pion and rho meson is presented in Sec. 14.7. The presentation in this chapter concludes in Sec. 14.8 with a general discussion of excited states based on an analysis by Landau. This

analysis relies on the use of exact sp propagators and presumes that the correlated ground state still maintains some of the properties of the Fermi gas and does not correspond to a superfluid or superconductor.

### 14.1 Polarization propagator

The relevant limit of the tp propagator to study excited states in many-fermion systems is given by

$$\begin{aligned} G_{ph}(\alpha, \beta^{-1}; \gamma, \delta^{-1}; t-t') &\equiv \lim_{t_\beta \rightarrow t'} \lim_{t_\gamma \rightarrow t'} G_{II}(\alpha t, \bar{\delta} t', \bar{\beta} t_\beta, \gamma t_\gamma) \\ &= -\frac{i}{\hbar} \langle \Psi_0^A | \mathcal{T}[b_{\beta_H}(t) a_{\alpha_H}(t) a_{\gamma_H}^\dagger(t') b_{\delta_H}^\dagger(t')] | \Psi_0^A \rangle \\ &= -\frac{i}{\hbar} \langle \Psi_0^A | \mathcal{T}[a_{\bar{\beta}_H}^\dagger(t) a_{\alpha_H}(t) a_{\gamma_H}^\dagger(t') a_{\bar{\delta}_H}(t')] | \Psi_0^A \rangle. \end{aligned} \quad (14.1)$$

The operators  $b$  and  $b^\dagger$  appear in order to be able to properly couple ph operators to good total angular momentum states for later applications. Consider the time-reversal operator which transforms sp states according to

$$\mathcal{T} |\alpha\rangle = |\bar{\alpha}\rangle. \quad (14.2)$$

It is useful to emphasize that this operator depends on the sp basis that is chosen [Sakurai (1994); Messiah (1999)] and requires the choice of a particular phase convention. For a particle with momentum  $\mathbf{p}$ , spin 1/2 (not explicitly shown), and spin projection  $m_s$  we choose the convention

$$\mathcal{T} |\mathbf{p}, m_s\rangle \equiv |\overline{\mathbf{p}}, \overline{m_s}\rangle = (-1)^{1/2+m_s} |-\mathbf{p}, -m_s\rangle, \quad (14.3)$$

which shows that in this basis time reversal is equivalent to the product of the parity operator and a rotation operator around the  $y$ -axis by an angle  $\pi$  [Sakurai (1994)]. Note that we have chosen the phase convention in Eq. (14.3) which follows [Bohr and Mottelson (1998)]. Employing this choice, one may then define operators that produce holes (using this basis) by

$$b_{\mathbf{p}, m_s}^\dagger \equiv a_{\overline{\mathbf{p}}, \overline{m_s}} = (-1)^{1/2+m_s} a_{-\mathbf{p}, -m_s}. \quad (14.4)$$

Whenever appropriate, the relevant phase convention and character of the time-reversal operator will be explicitly given. In the development of this section, the only reminder of this feature will be the appearance of the “bar” over sp quantum numbers indicating time-reversed states.

The presence in Eq. (14.1) of only two times in this limit of the tp propagator implies that only one energy variable is required upon Fourier transformation. In order to prepare for this Fourier transformation one may insert the definition of the Heisenberg removal and addition operators (Eqs. (8.3) and (8.4)) and the definition of the time-ordering operation in terms of step functions into Eq. (14.1). Inserting complete sets of  $A$  particle states at appropriate places then yields the following expression for  $G_{ph}$  in the usual way

$$\begin{aligned}
G_{ph}(\alpha, \beta^{-1}; \gamma, \delta^{-1}; t - t') &= -\frac{i}{\hbar} \langle \Psi_0^A | a_{\beta}^{\dagger} a_{\alpha} | \Psi_0^A \rangle \langle \Psi_0^A | a_{\gamma}^{\dagger} a_{\delta} | \Psi_0^A \rangle \quad (14.5) \\
&- \frac{i}{\hbar} \left\{ \sum_{n \neq 0} \theta(t - t') e^{\frac{i}{\hbar}(E_0^A - E_n^A)(t - t')} \langle \Psi_0^A | a_{\beta}^{\dagger} a_{\alpha} | \Psi_n^A \rangle \langle \Psi_n^A | a_{\gamma}^{\dagger} a_{\delta} | \Psi_0^A \rangle \right. \\
&\left. + \sum_{n \neq 0} \theta(t - t') e^{\frac{i}{\hbar}(E_0^A - E_n^A)(t' - t)} \langle \Psi_0^A | a_{\gamma}^{\dagger} a_{\delta} | \Psi_n^A \rangle \langle \Psi_n^A | a_{\beta}^{\dagger} a_{\alpha} | \Psi_0^A \rangle \right\},
\end{aligned}$$

where the contribution of the ground state has been explicitly isolated. Noting that the contribution of the first term in Eq. (14.5) involves matrix elements of the one-body density operator (Eq. 8.21) that are already contained in the sp propagator, it is conventional to introduce the so-called polarization propagator which only includes the contribution of excited states in Eq. (14.5)

$$\begin{aligned}
\Pi(\alpha, \beta^{-1}; \gamma, \delta^{-1}; t - t') &= G_{ph}(\alpha, \beta^{-1}; \gamma, \delta^{-1}; t - t') \\
&+ \frac{i}{\hbar} \langle \Psi_0^A | a_{\beta}^{\dagger} a_{\alpha} | \Psi_0^A \rangle \langle \Psi_0^A | a_{\gamma}^{\dagger} a_{\delta} | \Psi_0^A \rangle. \quad (14.6)
\end{aligned}$$

With this preparation one can now perform the Fourier transform of this polarization propagator to obtain its Lehmann representation by employing the integral representation of the step functions given by Eq. (7.7)

$$\begin{aligned}
\Pi(\alpha, \beta^{-1}; \gamma, \delta^{-1}; E) &= \int_{-\infty}^{\infty} d(t - t') e^{\frac{i}{\hbar}E(t - t')} \Pi(\alpha, \beta^{-1}; \gamma, \delta^{-1}; t - t') \\
&= \sum_{n \neq 0} \frac{\langle \Psi_0^A | a_{\beta}^{\dagger} a_{\alpha} | \Psi_n^A \rangle \langle \Psi_n^A | a_{\gamma}^{\dagger} a_{\delta} | \Psi_0^A \rangle}{E - (E_n^A - E_0^A) + i\eta} \\
&- \sum_{n \neq 0} \frac{\langle \Psi_0^A | a_{\gamma}^{\dagger} a_{\delta} | \Psi_n^A \rangle \langle \Psi_n^A | a_{\beta}^{\dagger} a_{\alpha} | \Psi_0^A \rangle}{E + (E_n^A - E_0^A) - i\eta}. \quad (14.7)
\end{aligned}$$

As in the case of the sp propagator, this polarization propagator contains important information in its denominator related to the position of excited states, here of the  $A$  particle system, and relevant transition amplitudes connecting the ground state with those excited states in the numerator. In particular, for the case of a one-body excitation operator  $\hat{O}$  given by

$$\hat{O} = \sum_{\alpha\beta} \langle \alpha | O | \beta \rangle a_{\alpha}^{\dagger} a_{\beta}, \quad (14.8)$$

the transition probability from the ground state to an excited state is given by

$$\begin{aligned} \left| \langle \Psi_n^A | \hat{O} | \Psi_0^A \rangle \right|^2 &= \sum_{\alpha\beta} \sum_{\gamma\delta} \langle \gamma | O | \delta \rangle \langle \Psi_n^A | a_{\gamma}^{\dagger} a_{\delta} | \Psi_0^A \rangle \\ &\times \langle \alpha | O | \beta \rangle^* \langle \Psi_n^A | a_{\alpha}^{\dagger} a_{\beta} | \Psi_0^A \rangle^*. \end{aligned} \quad (14.9)$$

This result demonstrates that the numerator of the first term in Eq. (14.7) contains the relevant transition amplitudes for a given state  $n$  to evaluate this transition probability. Examples of cases where this type of one-body excitation mechanism plays an important role, are given by inelastic electron scattering off nuclei and neutron scattering off condensed matter systems.

It is instructive to evaluate the noninteracting limit of the polarization propagator. This limit can be directly obtained from Eq. (14.6) by replacing  $\hat{H}$  by  $\hat{H}_0$  and  $|\Psi_0^A\rangle$  by the noninteracting ground state  $|\Phi_0^A\rangle$ .

$$\begin{aligned} \Pi^{(0)}(\alpha, \beta^{-1}; \gamma, \delta^{-1}; t - t') &= G_{ph}^{(0)}(\alpha, \beta^{-1}; \gamma, \delta^{-1}; t - t') \\ &+ \frac{i}{\hbar} \langle \Phi_0^A | a_{\beta}^{\dagger} a_{\alpha} | \Phi_0^A \rangle \langle \Phi_0^A | a_{\gamma}^{\dagger} a_{\delta} | \Phi_0^A \rangle \end{aligned} \quad (14.10)$$

By employing the sp basis in which  $H_0$  is diagonal, the states that can be excited then also correspond to eigenstates of  $\hat{H}_0$  as discussed in Sec. 3.1 with the following result

$$\hat{H}_0 a_{\gamma}^{\dagger} a_{\bar{\delta}} | \Phi_0 \rangle = \theta(\gamma - F) \theta(F - \bar{\delta}) \left\{ \varepsilon_{\gamma} - \varepsilon_{\bar{\delta}} + E_{\Phi_0^A} \right\} a_{\gamma}^{\dagger} a_{\bar{\delta}} | \Phi_0 \rangle, \quad (14.11)$$

where Kramer's degeneracy has been used in putting  $\varepsilon_{\bar{\delta}} = \varepsilon_{\delta}$ . One may leave out the bar over quantum numbers in the step functions for the same reason. Rewriting the interaction picture operators in terms of their explicit time dependence according to Eqs. (A.15) and (A.16) and evaluating the relevant expectation values w.r.t. the noninteracting ground state yields

the following expression for the noninteracting polarization propagator

$$\begin{aligned} \Pi^{(0)}(\alpha, \beta^{-1}; \gamma, \delta^{-1}; t - t') = & \\ & - \frac{i}{\hbar} \left\{ \theta(t - t') \theta(\alpha - F) \theta(F - \beta) \delta_{\alpha, \gamma} \delta_{\beta, \delta} e^{-i(\varepsilon_\alpha - \varepsilon_\beta)(t - t')/\hbar} \right. \\ & \left. + \theta(t' - t) \theta(F - \alpha) \theta(\beta - F) \delta_{\alpha, \gamma} \delta_{\beta, \delta} e^{-i(\varepsilon_\beta - \varepsilon_\alpha)(t' - t)/\hbar} \right\}, \quad (14.12) \end{aligned}$$

where time-reversed quantum numbers are replaced by the usual version since these states are usually equivalent. The first term in Eq. (14.12) corresponds to the independent propagation of a particle with quantum numbers  $\alpha$  ( $\gamma$ ) from  $t'$  to  $t$  and a hole with  $\beta$  ( $\delta$ ) from  $t$  to  $t'$ . The second term exchanges the role of  $t$  and  $t'$  as well as those of the sp quantum numbers and can be referred to as independent hole-particle (hp) propagation. Graphically this is illustrated in Fig. 14.1. It is customary to refer to part *a*) of Fig. 14.1 as forward propagation and part *b*) as backward propagation. This graphical representation in terms of noninteracting sp propagators is totally appropriate since a look at Eq. (8.32) demonstrates that up to a constant the two terms in Eq. (14.12) correspond exactly to such a product.

Using the integral representation [see Eq. (7.7)] of the step functions in Eq. (14.12) one can easily evaluate the *FT* of  $\Pi_{ph}^{(0)}$  to obtain

$$\begin{aligned} \Pi^{(0)}(\alpha, \beta^{-1}; \gamma, \delta^{-1}; E) = & \\ \delta_{\alpha, \gamma} \delta_{\beta, \delta} \left\{ \frac{\theta(\alpha - F) \theta(F - \beta)}{E - (\varepsilon_\alpha - \varepsilon_\beta) + i\eta} - \frac{\theta(F - \alpha) \theta(\beta - F)}{E + (\varepsilon_\beta - \varepsilon_\alpha) - i\eta} \right\}, \quad (14.13) \end{aligned}$$

shown graphically in Fig. 14.2. This simple structure of the noninteracting polarization propagator confirms that the location of its poles correspond to ph states that are obtained by removing a particle from an occupied level and placing it in an empty level of  $H_0$ . It should also be noted that the

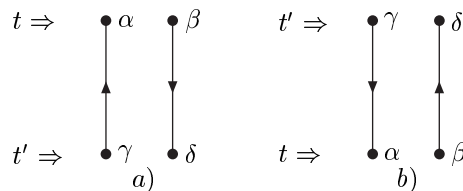


Fig. 14.1 Diagrammatic representation of the ph and hp propagation terms in Eq. (14.12) representing the unperturbed polarization propagator in the time formulation.

location of the poles in Eq. (14.13) is symmetric around  $E = 0$  which is a reminder that a pair of fermion operators have certain properties in common with bosons (see Ch. 12). The numerator of Eq. (14.13) reflects that the ph pair added to the noninteracting ground state must propagate without change for the chosen pair of quantum numbers. The exact polarization propagator in Eq. (14.7) does not share this property, in principle, and, in general, has nondiagonal contributions, as well as several excited states that can be reached by adding a ph pair with quantum numbers  $\gamma\delta^{-1}$  to the ground state.

It is a useful exercise to confirm that this noninteracting polarization propagator can also be obtained by considering the following convolution of noninteracting sp propagators

$$\begin{aligned}\Pi^{(0)}(\alpha, \beta^{-1}; \gamma, \delta^{-1}; E) &= \int \frac{dE'}{2\pi i} G^{(0)}(\alpha, \gamma; E + E') G^{(0)}(\bar{\beta}, \bar{\delta}; E') \\ &\equiv \delta_{\alpha, \gamma} \delta_{\beta, \delta} \Pi^{(0)}(\alpha, \beta^{-1}; E).\end{aligned}\quad (14.14)$$

The integral in Eq. (14.14) for each of four terms representing the product of the two noninteracting sp propagators can be evaluated by considering the distribution of the poles as a function of  $E'$ . When both poles occur on the same side of the real  $E'$ -axis the contour integral can be closed in the opposite half thereby rendering the corresponding contribution zero. For this reason only two terms survive the convolution in Eq. (14.14) representing ph or hp contributions as shown explicitly in Eq. (14.13). It is customary to refer to the first part of Eq. (14.13) as the forward-going term, and the second term as the backward-going one. Nevertheless it is also convenient in keeping with the Feynman diagram convention to introduce only one diagram in the energy formulation for this term as shown in Fig. 14.2.

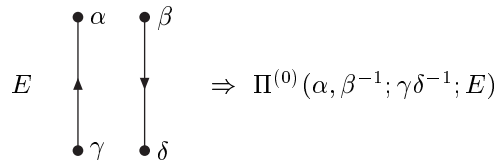


Fig. 14.2 Diagrammatic representation of the unperturbed polarization propagator in the energy formulation. Note that this Feynman diagram includes both ph and hp propagation terms as in Eq. (14.13).

## 14.2 Random Phase Approximation

Higher-order contributions to the polarization propagator can be evaluated by straightforward application of Wick's theorem. The relevant connected contributions have already been discussed in Sec. 10.3 for the more general case of four-time tp propagator. As in the analysis of this more general tp propagator, there are terms that represent an interaction between the initial and final ph state and terms that dress the noninteracting sp propagators. Both types of corrections appear in the first order contribution given by

$$\begin{aligned} \Pi^{(1)}(\alpha, \beta^{-1}; \gamma, \delta^{-1}; t - t') &= \left(\frac{-i}{\hbar}\right)^2 \int_{-\infty}^{\infty} dt_1 \frac{1}{4} \sum_{abcd} \langle ab | V | cd \rangle \quad (14.15) \\ &\times \langle \Phi_0^A | \mathcal{T} \left[ a_a^\dagger(t_1) a_b^\dagger(t_1) a_d(t_1) a_c(t_1) a_{\bar{\beta}}^\dagger(t) a_\alpha(t) a_\gamma^\dagger(t') a_{\bar{\delta}}(t') \right] | \Phi_0^A \rangle. \end{aligned}$$

in the time formulation. If the Hartree-Fock basis is employed these self-energy terms will vanish in first order. For the purpose of obtaining a scheme to calculate excited states using noninteracting sp propagators, it is therefore sufficient to consider only those contributions to Eq. (14.15) which link the propagators and discard terms with first-order self-energy insertions (as well as the truly disconnected terms). For the symmetrized version of  $V$  used in Eq. (14.15) one then obtains

$$\begin{aligned} \Pi^{(1)}(\alpha, \beta^{-1}; \gamma, \delta^{-1}; t - t') &\rightarrow (i\hbar)^2 \int_{-\infty}^{\infty} dt_1 \frac{1}{4} \sum_{abcd} \langle ab | V | cd \rangle \quad (14.16) \\ &\times G^{(0)}(\alpha, a; t - t_1) G^{(0)}(c, \bar{\beta}; t_1 - t) G^{(0)}(d, \gamma; t_1 - t') G^{(0)}(\bar{\delta}, b; t' - t_1). \end{aligned}$$

This result is illustrated in Fig. 14.3. For some systems it is useful to separate the direct and exchange contribution of the interaction  $V$  and treat them separately. For this reason, both terms are shown in Fig. 14.3. The physical interpretation of this term is now clear. Taking into account that the unperturbed sp propagators in Eq. (14.16) are diagonal in this sp basis, one obtains for this particular time-ordering  $t > t_1 > t'$  that a ph pair is added at time  $t'$  with quantum numbers  $\gamma\delta^{-1}$ , then propagation to  $t_1$  takes place. At this time an interaction changes to the propagation to a ph pair with quantum numbers  $\alpha\beta^{-1}$  which ends at  $t$  when this pair is removed. Since  $V$  contains both direct and exchange contribution, different diagrams can be associated with these two processes as shown in Fig. 14.3.

It is now convenient to introduce the ph version of the two-body matrix

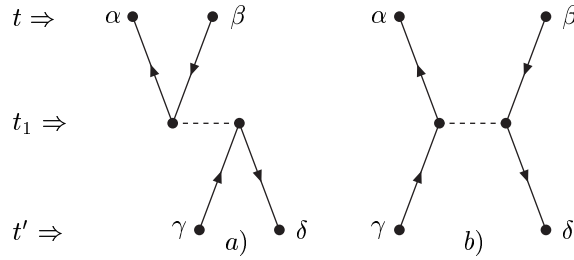


Fig. 14.3 Diagrammatic representation of the first-order correction to the polarization propagator in the time formulation. The time ordering  $t > t_1 > t'$  has been chosen for this picture. In part *a*) the direct contribution of the matrix element of the interaction is employed whereas in part *b*) the exchange part. The labels for the interaction have been suppressed for clarity.

element of  $V$  as follows

$$\langle \alpha \beta^{-1} | V_{ph} | \gamma \delta^{-1} \rangle \equiv \langle \alpha \bar{\delta} | V | \bar{\beta} \gamma \rangle. \quad (14.17)$$

This definition emphasizes the physical process, illustrated in Fig. 14.3 in which the interaction connects one ph pair with another. Using this definition and Fourier transforming Eq. (14.16) one obtains this first-order term in the energy formulation. This transformation is facilitated by using the inverse transforms of the sp propagators as given by Eq. (9.59). If the definition given in Eq. (14.14) is employed, this Fourier transform simplifies to

$$\Pi^{(1)}(\alpha, \beta^{-1}; \gamma, \delta^{-1}; E) = \Pi^{(0)}(\alpha, \beta^{-1}; E) \langle \alpha \beta^{-1} | V_{ph} | \gamma \delta^{-1} \rangle \Pi^{(0)}(\gamma, \delta^{-1}; E). \quad (14.18)$$

The corresponding diagrammatic representation is shown in Fig. 14.4 which is naturally similar to the one shown in Fig. 14.3. The analysis of this expression (or the equivalent one in the time formulation given by Eq. (14.16)) shows that there are four kinds of terms. In the language of the diagrams shown in Fig. 14.1 these correspond to forward-forward, forward-backward, backward-forward, and backward-backward contributions. The Feynman diagrams in Fig. 14.4 represents all four of these terms whereas Fig. 14.3 represents the forward-forward term in the time formulation. The pole structure of these first-order terms (in the interaction  $V_{ph}$ ) clearly does not correspond to the Lehmann representations of either the exact (Eq. (14.7)) or unperturbed (Eq. (14.13)) since they contain two poles. This problem has been encountered earlier when analyzing higher-order contributions to

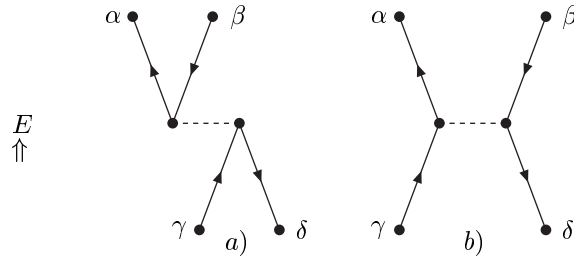


Fig. 14.4 Diagrammatic representation of the first-order correction to the polarization propagator in the energy formulation for both the direct *a*) and exchange *b*) process. The energy  $E$  labels the whole diagrams as indicated on the left side by the double arrow.

the sp propagator. In that case, the analysis produced the Dyson equation which generates for appropriate choices of the self-energy like those discussed in Chs. 11 and 13, a framework to generate approximate results that have the correct analytic properties associated with the Lehmann representation. The resulting Dyson equation is therefore a more appropriate vehicle to calculate sp properties. In addition, it may be interpreted as a Schrödinger equation for a particle in the medium. A similar analysis holds for the polarization propagator which also requires a similar infinite summation leading to a corresponding Schrödinger-like equation for ph propagation. One must therefore regard the sum of all contributions in which  $V_{ph}$  is iterated with  $\Pi^{(0)}$  as a minimum to obtain a polarization propagator which can be interpreted with a corresponding (though approximate) Lehmann representation. The analogy then corresponds to identifying  $V_{ph}$  for example with the lowest-order self-energy and  $\Pi^{(0)}$  with  $G^{(0)}$ . The summation of all these terms can be accomplished by rewriting the right-hand side of Eq. (14.18) as follows

$$\begin{aligned}
 & \Pi^{(0)}(\alpha, \beta^{-1}; E) \langle \alpha \beta^{-1} | V_{ph} | \gamma \delta^{-1} \rangle \Pi^{(0)}(\gamma, \delta^{-1}; E) = \\
 & \Pi^{(0)}(\alpha, \beta^{-1}; E) \sum_{\epsilon \theta} \langle \alpha \beta^{-1} | V_{ph} | \epsilon \theta^{-1} \rangle \Pi^{(0)}(\epsilon, \theta^{-1}; \gamma, \delta^{-1}; E) \\
 & \rightarrow \Pi^{(0)}(\alpha, \beta^{-1}; E) \sum_{\epsilon \theta} \langle \alpha \beta^{-1} | V_{ph} | \epsilon \theta^{-1} \rangle \Pi^{RPA}(\epsilon, \theta^{-1}; \gamma, \delta^{-1}; E).
 \end{aligned}
 \tag{14.19}$$

When this last expression is added to the noninteracting polarization propagator, one obtains the corresponding approximation to the exact polarization propagator in which the ph interaction  $V_{ph}$  is iterated to all or-

ders with the noninteracting polarization propagator in complete analogy with the Dyson equation that iterates the lowest-order self-energy contribution. This approximation yields the following equivalent equations [see Eq. (14.14)]

$$\begin{aligned} \Pi^{RPA}(\alpha, \beta^{-1}; \gamma, \delta^{-1}; E) &= \Pi^{(0)}(\alpha, \beta^{-1}; \gamma, \delta^{-1}; E) \\ &+ \Pi^{(0)}(\alpha, \beta^{-1}; E) \sum_{\epsilon\theta} \langle \alpha\beta^{-1} | V_{ph} | \epsilon\theta^{-1} \rangle \Pi^{RPA}(\epsilon, \theta^{-1}; \gamma, \delta^{-1}; E). \end{aligned} \tag{14.20}$$

and

$$\begin{aligned} \Pi^{RPA}(\alpha, \beta^{-1}; \gamma, \delta^{-1}; E) &= \Pi^{(0)}(\alpha, \beta^{-1}; \gamma, \delta^{-1}; E) \\ &+ \sum_{\epsilon\theta\zeta\xi} \Pi^{(0)}(\alpha, \beta^{-1}; \zeta\xi^{-1}; E) \langle \zeta\xi^{-1} | V_{ph} | \epsilon\theta^{-1} \rangle \Pi^{RPA}(\epsilon, \theta^{-1}; \gamma, \delta^{-1}; E). \end{aligned} \tag{14.21}$$

By successively replacing  $\Pi^{RPA}$  on the right side of Eq. (14.20) [or Eq. (14.21)] by the corresponding expression given by this right-hand side, one may convince oneself that one generates all higher-order terms in which unperturbed ph propagation is interrupted by the action of  $V_{ph}$  by zero, one, two, three, etc. many times. This particular sum of terms is known in the many-body literature as the random phase approximation (RPA) and the corresponding label has been used in Eqs. (14.19) - (14.21). The diagrammatic representation of Eq. (14.21) is given in Fig. 14.5.

The diagrams that are generated by this approximation to the polarization propagator have various names in the literature, having been called

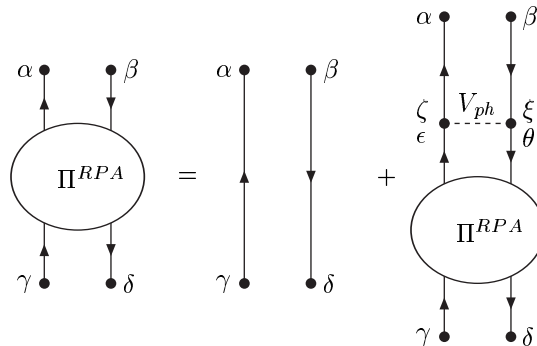


Fig. 14.5 Diagrammatic representation of the second equality in Eq. (14.21). Note that the dashed line represents  $V_{ph}$  as defined in Eq. (14.17).

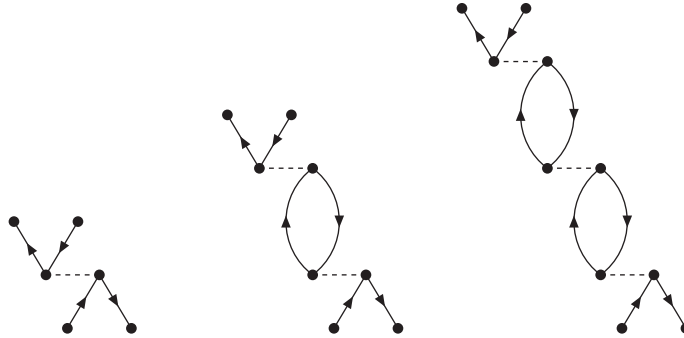


Fig. 14.6 Diagrammatic representation of a few higher-order diagrams generated by Eq. (14.21) when only the direct contribution to  $V_{ph}$  is employed as shown in Fig. 14.4. Note that the dashed line in this figure represents the corresponding direct contribution to  $V_{ph}$  as defined in Eq. (14.17).

ring, bubble, or sausage diagrams. This name calling becomes clear when the direct contribution to  $V_{ph}$  is used to generate the higher-order terms implied by Eq. (14.21). Examples of such diagrams are shown in Fig. 14.6. The bubbles or rings emerge when the direct part of the interaction is used to connect the unperturbed ph propagation as shown in Fig. 14.6. It should be emphasized again that the diagrams displayed in Fig. 14.6 correspond to Feynman diagrams in the energy formulation. Each bubble, for example, represents the sum of a forward- and a backward-going term corresponding to the first or second term of Eq. (14.13), respectively. The presence of both these terms implies an interplay between these components when Eq. (14.21) is solved. The presence of both terms generates the possibility of intermediate states in which many particle-hole states are present at the same time. If no backward-going contributions are present only one particle-hole pair propagates at each moment. One can generate an example of a term with more intermediate particle-hole states by taking one of the bubbles in Fig. 14.6 and flipping it downward. The presence of such contributions implies that some higher-order contributions with more particle-hole intermediate states are included. Other are, however, neglected in particular those in which particles or holes are exchanged with each other. One may argue that these Pauli exchange terms add up with random phases and might therefore be rather small, hence the appearance of the name random phase approximation. General features of the solutions

of the RPA equation for the polarization propagator in finite systems will be presented in the next section.

### 14.3 RPA in finite systems and the schematic model

The solution to Eq. (14.20) starts by assuming that  $\Pi^{RPA}$  also has a Lehmann representation just as the unperturbed and the exact polarization propagator. This assumption implies that the transition amplitudes and excitation energies in principle require a distinct notation since they refer to a specific approximation (RPA) to the polarization propagator. It is convenient to define

$$\mathcal{Z}_{\alpha\beta}^n \equiv \langle \Psi_n^A | a_\alpha^\dagger a_\beta | \Psi_0^A \rangle \quad (14.22)$$

and

$$\varepsilon_n^\pi \equiv E_n^A - E_0^A, \quad (14.23)$$

keeping in mind that these quantities refer to the RPA description of the polarization propagator. With this notation the corresponding Lehmann representation becomes

$$\Pi^{RPA}(\alpha, \beta^{-1}; \gamma, \delta^{-1}; E) = \sum_{n \neq 0} \frac{(\mathcal{Z}_{\alpha\beta}^n)^* \mathcal{Z}_{\gamma\delta}^n}{E - \varepsilon_n^\pi + i\eta} - \sum_{n \neq 0} \frac{(\mathcal{Z}_{\delta\gamma}^n)^* \mathcal{Z}_{\beta\alpha}^n}{E + \varepsilon_n^\pi - i\eta}. \quad (14.24)$$

In the case of a finite system it is natural to consider bound excited states and, consequently, the summation in Eq. (14.24) indeed involves some discrete states. As a result, this Lehmann representation includes simple poles. For simplicity one may assume that all excited states correspond to discrete excitation energies. With this assumption one may exploit a technique that was introduced in Ch. 7 (and used several times since) to solve propagator equations with discrete poles. The procedure involves the calculation of

$$\lim_{E \rightarrow \varepsilon_n^\pi} (E - \varepsilon_n^\pi) \{ \Pi^{RPA} = \Pi^{(0)} + \Pi^{(0)} V_{ph} \Pi^{RPA} \}, \quad (14.25)$$

where Eq. (14.21) has been rendered in a schematic fashion. As in Ch. 7, one proceeds by considering the limits for the three terms in Eq. (14.25). Using the Lehmann representation for  $\Pi^{RPA}$ , one immediately obtains the product of two transition amplitudes associated with excited state  $n$  for the left hand side of Eq. (14.25). The limit yields no contribution when it is taken for the first term on the right side which involves  $\Pi^{(0)}$ . One may draw